

("green pigments") could be formed by such a transfer mechanism.¹⁸

Registry No. 1a, 83219-57-2; 1b, 79197-95-8; 1c, 70936-44-6; 2a, 83219-58-3; 2b, 83219-60-7; 2c, 83219-61-8; 3a, 83219-59-4; 3b, 51552-53-5; 3c, 81856-91-9; Fe^{III}(TPP)(Cl), 16456-81-8.

(18) So far, most *N*-alkylporphyrins found in vivo as "green pigments" in the liver were derived from the oxidative activation of exogenous compounds containing an easily accessible double or triple carbon-carbon bond.¹⁹

(19) (a) Ortiz de Montellano, R. E.; Kunze, K. L.; Mico, B. A. *Mol. Pharmacol.* 1980, 18, 602. (b) Ortiz de Montellano, R. E.; Mico, B. A. *Ibid.* 1980, 18, 128. (c) Ortiz de Montellano, R. E.; Beilan, H. S.; Kunze, K. L.; Mico, B. A. *J. Biol. Chem.* 1981, 256, 4395.

(20) Note Added in Proof: During the submission of this paper, a paper appeared describing the transfer of the phenyl group of Fe(TPP)(Ph) from iron to nitrogen upon treatment of this complex by O₂ and acids: Ortiz de Montellano, R. E.; Kunze, K. L.; Augusto, O. *J. Am. Chem. Soc.* 1982, 104, 3545.

Osmium(IV)-Mediated Oxidative Dehydrogenation of Coordinated Amines: Crystal and Molecular Structures of *cis*-1,2-Ethanediaminebis(1,2-ethanediaminato(1-))-osmium(IV) Dibromide

Peter A. Lay,¹ Alan M. Sargeson,*¹ Brian W. Skelton,² and Allan H. White²

The Research School of Chemistry
The Australian National University
Canberra, ACT 2600, Australia
and The School of Chemistry
The University of Western Australia
Nedlands, WA 6009, Australia

Received May 27, 1982

The Os(IV) complexes [Os(en)(en-H)₂]²⁺ and [Os(en)₂(en-H)]³⁺ were originally prepared by Dwyer and Hogarth^{3,4} and formulated as diamagnetic Os(IV) 1,2-ethanediamine complexes deprotonated at the N centers. An alternative interpretation would have been diamagnetic osmium(II) imine complexes. This reinvestigation stemmed from the recognition by Basolo et al.⁵ that the complex formulated⁶ as [Ru(en-H)₂(en-2H)]²⁺ was in fact the Ru(II) complex [Ru(en)₂(diim)]²⁺. An X-ray crystallographic study of the complex [Os(en)(en-H)₂]Br₂⁷ (Figure 1) has now substantiated the original interpretation.⁴ The complex cation has an octahedrally distorted Os^{IV}N₆ core, with two mononegative aminate ions (on different ligands) occupying a *cis* configuration. The short Os-N (aminate) bonds (1.90 Å), as compared to the Os-N (amine) bonds, 2.11 Å (*cis*) and 2.19 Å (*trans*), are attributed to donation of electron density from filled p_z orbitals of the ligands to empty d orbitals on Os(IV), giving effectively two Os-N double bonds. The conclusion is supported by the increase in angle between the double bonds (110°) and the consequent narrowed N-Os-N angle (76°) for the en chelate *trans* to the *cis*

Table I. Atomic Coordinates for *cis*-[Os(en)(en-H)₂]Br₂

atom	x	y	z
Cation			
Os	0.00000 (-)	0.21515 (6)	0.25000 (-)
Axial Ligand			
N	-0.0950 (5)	-0.0134 (9)	0.1973 (6)
H _N (A)	-0.132 (8)	-0.017 (15)	0.106 (12)
H _N (B)	-0.143 (11)	0.039 (24)	0.200 (16)
C	-0.0407 (6)	-0.1772 (11)	0.2568 (9)
H _C (A)	-0.079 (6)	-0.284 (12)	0.221 (9)
H _C (B)	-0.005 (7)	-0.187 (14)	0.369 (10)
Other Ligand			
N	0.1120 (5)	0.3588 (10)	0.3319 (7)
H _N	0.146 (5)	0.372 (10)	0.310 (7)
C	0.1601 (6)	0.4129 (11)	0.4687 (8)
H _C (A)	0.218 (6)	0.329 (13)	0.529 (9)
H _C (B)	0.180 (7)	0.543 (15)	0.467 (10)
C'	0.0866 (6)	0.4007 (12)	0.4947 (8)
H _{C'} (A)	0.121 (6)	0.411 (12)	0.579 (8)
H _{C'} (B)	0.033 (6)	0.507 (12)	0.449 (9)
N'	0.0324 (5)	0.2335 (10)	0.4371 (6)
H _{N'} (A)	0.072 (7)	0.138 (16)	0.489 (10)
H _{N'} (B)	-0.012 (6)	0.224 (11)	0.448 (8)
Anion			
Br	0.18660 (6)	0.11325 (13)	0.12672 (8)

Table II. Cation Geometry^a

(a) Osmium Coordination Environment ^b						
	r _{Os-N}	N	N'	N _{ax}	N	N'
N _{ax}	2.194 (7)	161.7 (3)	92.5 (3)	76.0 (3)	87.4 (3)	93.5 (3)
N	1.896 (7)		81.0 (4)	87.4 (3)	110.0 (3)	94.6 (3)
N'	2.113 (9)			93.5 (3)	94.6 (3)	172.5 (3)
(b) Ligand Geometries						
ligand	"axial"	"equatorial"				
Distances (Å)						
N-C	1.46 (1)	1.48 (1)				
N'-C'		1.48 (1)				
C-C(1)	1.52 (2)	1.49 (2)				
Angles (deg)						
Os-N-C	112.3 (5)	118.6 (7)				
Os-N'-C'		106.3 (7)				
N-C-C(1)	106.8 (9)	107.2 (6)				
N'-C'-C		108.0 (9)				

^a Atoms generated by the 2-fold rotor are italicized. ^b r is the metal ligand distances (Å). Other entries in the matrix are the angles subtended at the osmium by the relevant atoms.

aminate ions, together with the location and refinement in (x, y, z) of all hydrogen atoms (Tables I and II).

Stable Os(IV) ammine complexes are rare,⁸ and the stabilization in this instance apparently arises from the donation of electron density to the Os(IV) center. The effect is seen dramatically in the redox potentials for the singly (+0.29V vs. Ag/AgCl/saturated LiCl (acetone) electrode in acetone) and double deprotonated (~-1.2 V) ions. The difference of >1 V cannot be attributed to just the change in charge. Comparable effects for Co(III) ammine complexes lead to redox potential differences in the range 0.1-0.2 V.⁹ Similar large stabilizations of M(IV) species have been noted by deprotonation of amines coordinated to Pt(IV),⁹ but here the ability of d⁶ Pt(IV) to accept electrons from the ligand is more questionable and needs to be observed structurally. The large effects are consistent, however, with the sets of lone pairs of electrons donating charge to the Os(IV) ion in a very substantial

(8) Stable complexes of Os(IV) with an N₄X₂ chromophore have been isolated previously, but [Os^{IV}(NH₃)₅L]ⁿ⁺ and [Os(NH₃)₆]⁴⁺ were reported to be very unstable. Buhr, J. D.; Winkler, J. R.; Taube, H. *Inorg. Chem.* 1980, 19, 2416-2425.

(9) Lay, P. A. Ph.D. Thesis, Australian National University, Aug 1981.

(1) The Australian National University.

(2) The University of Western Australia.

(3) Ligand abbreviations: en = 1,2-ethanediamine; en-H = 1,2-ethanediaminate(1-); en-2H = 1,2-ethanediaminate(2-); im = 2-aminoethanimine; diim = ethanediiimine; Me₂diim = 2,3-butanediimine; bpy = 2,2'-bipyridine; ampy = 2-(aminomethyl)pyridine; impy = 2-(iminomethyl)pyridine; hepy = 2-(1-hydroxyethyl)pyridine.

(4) Dwyer, F. P.; Hogarth, J. W. *J. Am. Chem. Soc.* 1953, 75, 1008-1009; 1955, 77, 6152-6154.

(5) Lane, B. C.; Lester, J. E.; Basolo, F. J. *Chem. Soc., Chem. Commun.* 1971, 1618-1619.

(6) Elsbernd, H.; Beattie, J. K. *J. Chem. Soc. A* 1970, 2598-2600.

(7) Anal. for C₈H₂₂Br₂N₆Os, C, H, Br, N. ¹³C NMR (D₂O) -23.8 ppm vs. dioxane as internal reference.

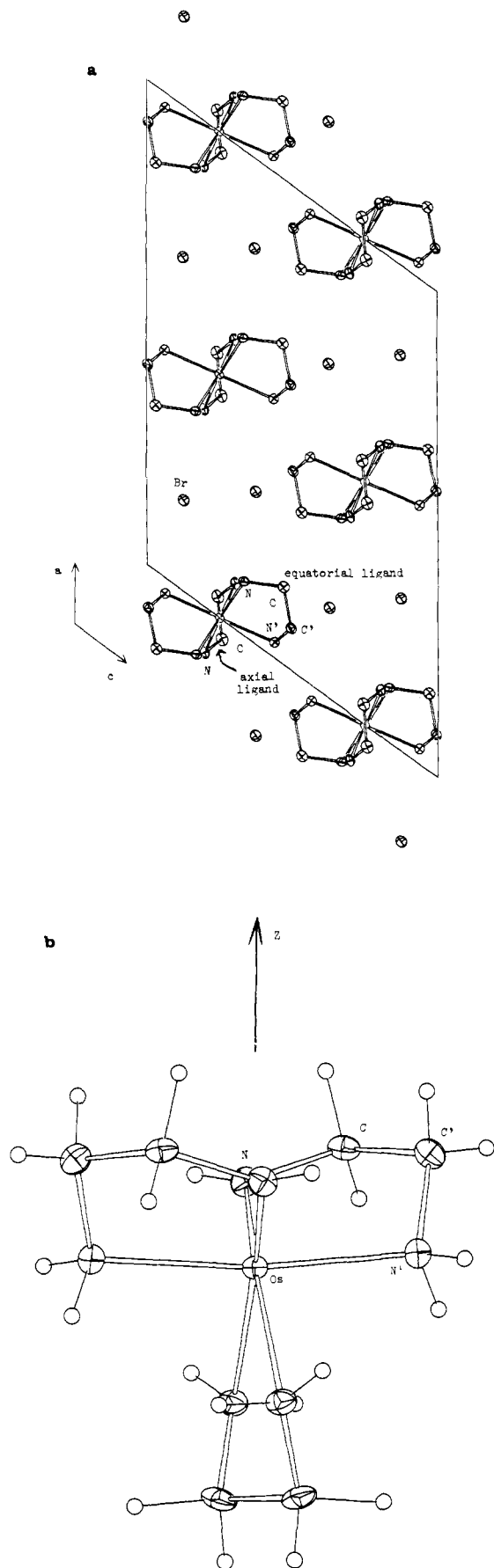
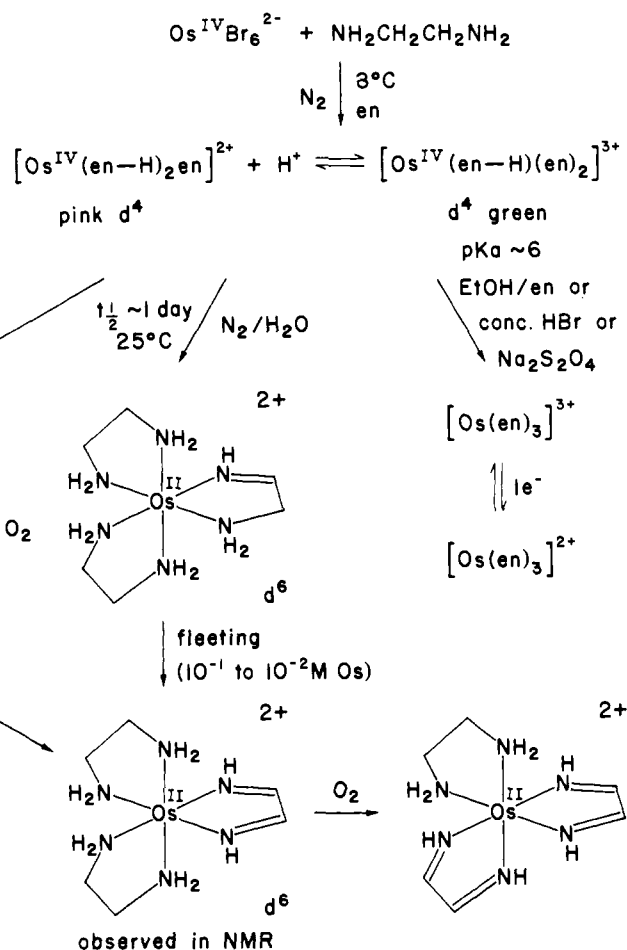


Figure 1. Projection of $[\text{Os}(\text{en})(\text{en-H})_2]\text{Br}_2$ showing (a) the unit cell contents and (b) the cation down and normal to the crystallographic b axis, respectively. Thermal ellipsoids are shown at the 20% probability level, and in (b) the hydrogen atoms have an arbitrary radius of 0.1 Å.

Scheme I



manner. Using the magnitude of these effects and the failure to observe oxidation of $[\text{Os}(\text{en})_3]^{3+}$ to $[\text{Os}(\text{en})_3]^{4+}$ in aqueous solution, we estimate the $[\text{Os}(\text{en})_3]^{4+/3+}$ potential to be $\geq +2$ V. This is also consistent with an observation of an oxidation wave at $\sim +2$ V vs. Ag/AgCl/0.1 M LiCl acetone electrode in acetone or acetonitrile (Au electrode).

The amine protons on the $[\text{Os}(\text{en})_2(\text{en-H})]\text{Br}_3 \cdot 3\text{H}_2\text{O}$ complex¹⁰ are acidic ($\text{p}K_a$ 5.8)⁴ and are not observed by ^1H NMR spectroscopy in D_2O or DCl. Also the ^{13}C NMR spectra of the $[\text{Os}(\text{en})_2(\text{en-H})]^{3+}$ and $[\text{Os}(\text{en})(\text{en-H})_2]^{2+}$ ions^{7,10} showed only one signal, which is consistent with equivalent carbon atoms on the NMR time scale and rapid exchange of the protons among the nitrogen sites.

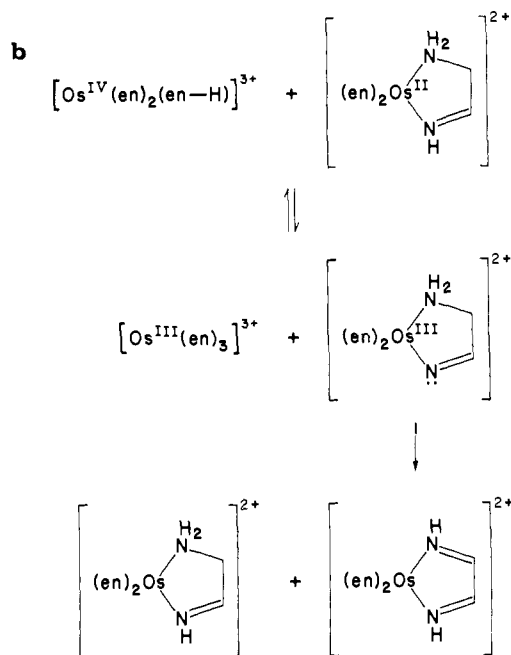
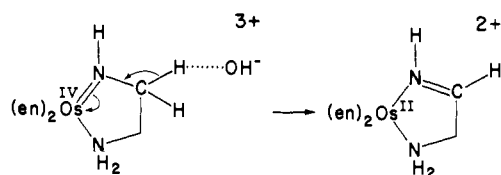
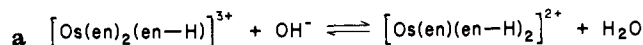
Under N_2 , the Os(IV) complexes were observed to undergo spontaneous oxidative dehydrogenation of the ligand to form an Os(II) imine species ($\epsilon_{400}^{\text{max}} \sim 10^4 \text{ M}^{-1} \text{ cm}^{-1}$). The reaction was followed spectrophotometrically at 400 nm and pH 7.0 ($\text{NaH}_2\text{PO}_4/\text{Na}_2\text{HPO}_4$, 10^{-4} M $[\text{Os}(\text{en})(\text{en-H})_2]\text{Br}_2$, μ 0.20 M, (NaCF_3SO_3), 25°C) and was first order ($k_{\text{obsd}} \sim 10^{-5} \text{ s}^{-1}$). In more concentrated solutions (10^{-2} to 10^{-1} M), with use of ^1H and ^{13}C NMR spectroscopy under an N_2 atmosphere, the major imine species obtained was the diimine $[\text{Os}(\text{en})_2(\text{diim})]^{2+}$ ion.¹² In the presence of O_2 , the $[\text{Os}(\text{en})_2(\text{im})]^{2+}$ complex was oxidized to $[\text{Os}(\text{en})_2(\text{diim})]^{2+}$ over ~ 1 day. The latter complex was more slowly oxidized over ~ 1 week to the tetraimine species, which was crystallized from aqueous HCl as $[\text{Os}(\text{en})(\text{diim})_2]\text{Cl}_2 \cdot \text{HCl} \cdot \text{H}_2\text{O}$.¹³

(10) Anal. for $\text{C}_6\text{H}_{29}\text{Br}_3\text{N}_6\text{O}_3\text{Os}$, C, H, N, ^{13}C NMR (0.1 M DCl) -29.9 ppm.

(11) Perrin, D. D. *Aust. J. Chem.* **1963**, *16*, 572-578.

(12) ^1H NMR (D_2O) δ 7.57 (CH=NH); ^{13}C NMR (D_2O) +94.9 (diim), -18.1 , -18.3 (en) ppm; vis/UV (H_2O) $\epsilon_{\text{max}}^{420} \sim 10^4 \text{ M}^{-1} \text{ cm}^{-1}$.

Scheme II



This chemistry is summarized in the reaction Scheme I, and the mechanism for the dehydrogenation is outlined in Scheme II. $[\text{Os}(\text{en})_2(\text{en}-\text{H})]^{3+}$ is stable in acid, although it is slowly reduced to $[\text{Os}(\text{en})_3]^{3+}$ in concentrated HBr solutions, and the $[\text{Os}(\text{en})(\text{en}-\text{H})_2]^{2+}$ ion is stabilized (in the absence of O_2) as the pH increases. Optimum spontaneous oxidation of the ligand to the monimine group at low (10^{-4} M) concentrations of complex appears to occur in the pH region of 6–7. Moreover, the imine CH protons do not exchange with deuterium when the oxidation is performed in D_2O , which indicates that the removal of the methylene proton and electron transfer are concerted. A combination of the increased acidity of the methylene protons and increased oxidizing power of the Os(IV) center in $[\text{Os}(\text{en})_2(\text{en}-\text{H})]^{3+}$ in comparison to $[\text{Os}(\text{en})(\text{en}-\text{H})_2]^{2+}$ is the driving force to the oxidation and explains the retardation by acid and base in Scheme IIa.

In the higher concentrations of Os employed in NMR experiments, it appears that the initially formed $[\text{Os}(\text{en})_2(\text{im})]^{2+}$ undergoes a cross reaction with $[\text{Os}(\text{en})_2(\text{en}-\text{H})]^{3+}$ to form $[\text{Os}(\text{en})_2(\text{im})]^{3+}$, which disproportionates to $[\text{Os}(\text{en})_2(\text{im})]^{2+}$ and $[\text{Os}(\text{en})_2(\text{diim})]^{2+}$. This explains the observation of $[\text{Os}(\text{en})_2(\text{diim})]^{2+}$ in the NMR experiments in contrast to the more dilute solutions. (Scheme IIb).

These results implicate the M(IV) oxidation state as an intermediate in the documented oxidative dehydrogenations of

(13) Anal. for $\text{C}_6\text{H}_{19}\text{Cl}_3\text{N}_6\text{O}_6$, C, H, Cl. ^1H NMR (D_2O) δ 2.61, 2.93 (br, 2, CH_2), \sim 4.8 (br, NH_2 , partially obscured by HDO peak), 6.41 (br, 1, NH_2), 8.51, 8.58 (s, 2, $\text{CH}=\text{NH}$, weak ABX coupling pattern), 11.65, 14.07 (br, 2, $\text{CH}=\text{NH}$), two CH_2 and two NH_2 peaks due to different chemical shifts of axial and equatorial protons; ^{13}C NMR (D_2O) +102.8 (trans, $\text{CH}=\text{NH}$); +97.7 (cis, $\text{CH}=\text{NH}$), -18.6 (en); IR (KBr disc) 1478 (vs), 1783 (vs) cm^{-1} ($\text{CH}=\text{NH}$); vis/UV (H_2O) $\epsilon_{380}^{\text{max}}$ 4500 $\text{M}^{-1}\text{cm}^{-1}$ (sh), $\epsilon_{423}^{\text{max}}$ 14100 $\text{M}^{-1}\text{cm}^{-1}$, $\epsilon_{500}^{\text{max}}$ 6000 $\text{M}^{-1}\text{cm}^{-1}$ (sh), $\epsilon_{653}^{\text{max}}$ 75 $\text{M}^{-1}\text{cm}^{-1}$.

ligands coordinated to Fe^{14} and Ru^{15} . It is becoming apparent that such intermediates may arise from base-catalyzed disproportionation of Ru(III) and Os(III) amine complexes to form M(II) and M(IV) species in other reactions.^{16,17} Of particular relevance is the oxidative dehydrogenation of the 2-(1-hydroxyethyl)pyridine ligand (hepy) in $[\text{Ru}(\text{NH}_3)_4(\text{hepy})]^{3+}$ to form the ketone analogue.¹⁷ This has been shown to occur by base-catalyzed disproportionation of the Ru(III) complex to Ru(II) and deprotonated Ru(IV) species. The latter undergoes oxidative dehydrogenation of the ligand. Kinetic experiments involving the oxidative dehydrogenation of the 2-(aminomethyl)pyridine ligand (ampy) in $[\text{Ru}(\text{bpy})_2(\text{ampy})]^{3+}$ have led to similar conclusions, i.e., an initial base-catalyzed disproportionation of Ru(III) to Ru(II) and Ru(IV).¹⁸ Preliminary work on the oxidative dehydrogenation of the 1,2-ethanediamine ligands of $[\text{Os}(\text{en})_3]^{3+}$ has led us to believe that a similar mechanism is operating here.¹⁹

The stabilization of the deprotonated Os(IV) complexes clearly arises from the donation of charge from the ligand to the metal. This is evident from the crystal structure and redox properties. It leads to bond orders greater than 1 for the Os–N bonds, and the unsaturation apparently increases the acidities of the adjacent methylene protons. There is a crude analogy with imine or carbonyl chemistry where similar increases in acidities are well-known. These effects could be expected to increase in the order $\text{Fe} \ll \text{Ru} < \text{Os}$, since this is the order of radial extension of the d orbitals.²⁰ Thus the M(IV) oxidation state would be less accessible (i.e., stronger oxidant) for Ru and more particularly Fe, thereby being much shorter lived and not generally observed as an intermediate in oxidative dehydrogenation processes. However, the importance of the relative energies of the empty d orbitals of the metal and the filled amine p orbitals needs also to be considered, and we are not certain as to which effect is most important.

The changes in stability of the II and III oxidation states of the Fe group on addition of imines into the coordination sphere has been ascribed to a similar phenomenon, whereby electron density in filled d orbitals on the metal is donated to empty π^* orbitals of the ligand. The degree of stabilization of the M(II) state again increases in the order $\text{Fe} \ll \text{Ru} < \text{Os}$.²⁰ This is dramatically shown by the potential of the 2+/3+ couple of $[\text{Os}(\text{en})_3]^{3+/2+}$ (–0.52 V) (prepared by $\text{Na}_2\text{S}_2\text{O}_4$,⁴ EtOH/en or concentrated HBr reduction of the Os(IV) complexes), in comparison to the $[\text{Os}(\text{en})(\text{diim})_2]^{3+/2+}$ (+0.69V) and the *trans*- $[\text{Os}(\text{NH}_3)_2(\text{Me}_2(\text{diim})_2)]^{3+/2+}$ couples +0.77 V²¹ vs. the standard hydrogen electrode.

Crystal data are as follows: $\text{C}_6\text{H}_{24}\text{Br}_2\text{N}_6\text{O}_6$; M_r 530.3; monoclinic; space group $C2/c$ (C_{2h}^2 , No. 15); $a = 17.256$ (8), $b = 7.566$ (3), $c = 12.802$ (5) Å; $\beta = 126.71$ (2)°, $U = 1339$ (1) Å³; D_c ($Z = 4$) = 2.63 g cm^{-3} ; μ_{Mo} = 150 cm^{-1} , $T = 295$ K, $F(000) = 992$. A unique data set was measured within the limit $2\theta_{\text{max}} = 55^\circ$, yielding 1951 independent reflections. 1617 of these with

(14) Goedken, V. L. *J. Chem. Soc., Chem. Commun.* **1972**, 207–208. Christoph, G. G.; Goedken, V. L. *J. Am. Chem. Soc.* **1973**, *95*, 3869–3875. Dabrowiak, J. C.; Busch, D. H. *Inorg. Chem.* **1975**, *14*, 1881–1888. Dabrowiak, J. C.; Lovocchio, F. V.; Goedken, V. L.; Busch, D. H. *J. Am. Chem. Soc.* **1972**, *94*, 5502–5504. Goedken, V. L.; Busch, D. H. *Ibid.* **1972**, *94*, 7355–7363. Krumholz, P. *Ibid.* **1953**, *75*, 2163–2166.

(15) Mahoney, D. F.; Beattie, J. K. *Inorg. Chem.* **1973**, *12*, 2561–2565. Brown, G. M.; Weaver, T. R.; Keene, F. R.; Meyer, T. J. *Ibid.* **1976**, *15*, 190–196. McWhinnie, W. R.; Miller, J. D.; Watts, J. B.; Waddan, D. Y. *Inorg. Chim. Acta* **1973**, *7*, 461–466. Diamond, S. E.; Tom, G. M.; Taube, H. *J. Am. Chem. Soc.* **1975**, *97*, 2661–2664. Keene, F. R.; Salmon, D. J.; Meyer, T. J. *Ibid.* **1976**, *98*, 1884–1889. Geungerich, C. P.; Schug, K. *Ibid.* **1977**, *99*, 3298–3302. Alvarez, V. E.; Allen, R. G.; Matsubara, T.; Ford, P. C. *Ibid.* **1974**, *96*, 7686–7692. Warren, L. F. *Inorg. Chem.* **1977**, *16*, 2814–2819.

(16) Rudd, DeF. P.; Taube, H. *Inorg. Chem.* **1971**, *10*, 1543–1544. Buhr, J. D.; Taube, H. *Ibid.* **1979**, *18*, 2208–2212. Thompson, M. S.; Meyer, T. J. *J. Am. Chem. Soc.* **1981**, *103*, 5577–5579.

(17) Tovrog, B. S.; Diamond, S. E.; Mares, F. *J. Am. Chem. Soc.* **1979**, *101*, 5067–5069.

(18) Ridd, M. J.; Keene, F. R. *J. Am. Chem. Soc.* **1981**, *103*, 5733–5740.

(19) Lay, P. A.; Sargeson, A. M., to be submitted for publication.

(20) Taube, H. *Surv. Prog. Chem.* **1973**, *6*, 1–46.

(21) Evans, I. P.; Everett, G. W.; Sargeson, A. M. *J. Am. Chem. Soc.* **1976**, *98*, 8041–8046.

$I > 3\sigma(I)$ were used in the full-matrix least-squares refinement after analytical absorption correction. Non-hydrogen atoms were refined in (x, y, z, U_{ij}) and hydrogen atoms in (x, y, z, U) . At convergence R, R' were 0.039 and 0.047, reflection weights being $(\sigma^2(F_o) + 0.0005(F_o)^2)^{-1}$. Neutral atom scattering factors were used, those for the non-hydrogen atoms being corrected for anomalous dispersion $(f'f'')$.²² Computation was carried out by using the X-RAY 76 program system²³ implemented by S. R. Hall on a Perkin-Elmer 3240 computer.

Acknowledgment. We are grateful for assistance from the ANU Microanalytical Section and the RSC NMR Service.

Registry No. $[\text{Os}^{\text{IV}}(\text{en-H})_2(\text{en})]^{2+}$, 16923-53-8; $[\text{Os}^{\text{IV}}(\text{en-H})(\text{en})_2]^{3+}$, 83095-58-3; $[\text{Os}(\text{en})_2(\text{im})]^{2+}$, 83095-59-4; $[\text{Os}(\text{en})_2(\text{diim})]^{2+}$, 83095-60-7; $[\text{Os}(\text{en})(\text{diim})_2]^{2+}$, 83095-61-8; $[\text{Os}(\text{en})_3]^{3+}$, 46138-85-6; $(\text{NH}_4)_2\text{Os-Br}_6$, 24598-62-7.

Supplementary Material Available: Listing of structure factor amplitudes (observed and calculated) and thermal parameters (1 page). Ordering information is given on any current masthead page.

(22) "International Tables for X-ray Crystallography"; Ibers, J. A., Hamilton, W. C., Eds.; Kynoch Press: Birmingham, 1974; Vol. 4.

(23) "The X-RAY System—Version of March, 1976", Technical Report TR-446, Computer Science Center, University of Maryland, Stewart, J. M., Ed.

(24) Conventional C, H, N analyses using an automatic analyzer gave consistently low N values for these osmium complexes. It is necessary to use the Kirsten-Dumas method in order to obtain satisfactory N analyses.

Total Synthesis of the C19–C29 Aliphatic Segment of (+)-Rifamycin S¹

S. Hanessian,* J.-R. Pougny, and I. K. Boessenkool

Department of Chemistry, University of Montreal
Montreal, Québec, Canada H3C 3V1

Received May 11, 1982

Among the landmark achievements in natural product synthesis in 1980 was Kishi's conquest of the rifamycin S structure.² In considering synthetic approaches³ to this formidable target,⁴ one is faced with several challenging problems, not the least of which is the construction of the sequence of alternating methyl and hydroxyl groups situated in the C19–C29 aliphatic segment and encompassing eight contiguous asymmetric centers. We report on the assembly of the aliphatic segment of rifamycin S based on a strategy that recognizes *hidden carbohydrate-type symmetry*⁵ as illustrated in Scheme I. Bond disconnection at C24–C25 generates two segments representing C19–C24 and C25–C29, which can be related to two "chiral templates"⁵ derived from D-glucose and designated as precursors A and B.

Precursor A. The synthesis of precursor A as shown in Scheme II starts with the readily available and crystalline epoxide **1**,⁶ which

(1) Portions of this work were presented at the Euechem Conference on "Uses of Carbohydrates as Starting Materials for Organic Synthesis", Belle-Ile-en-Mer, France, June 3–6, 1979; Euechem Stereochemistry Conference, Bürgenstock, Switzerland, April 27–May 3, 1980; 28th IUPAC Congress, Vancouver, Canada, August 16–21, 1981, OR 088.

(2) Nagaoka, H.; Rutsch, W.; Schmid, G.; Johnson, M. R.; Kishi, Y. *J. Am. Chem. Soc.* **1980**, *102*, 7962–7965. Iio, H.; Nagaoka, H.; Kishi, Y. *Ibid.* **1980**, *102*, 7965–7967. See also ref 22.

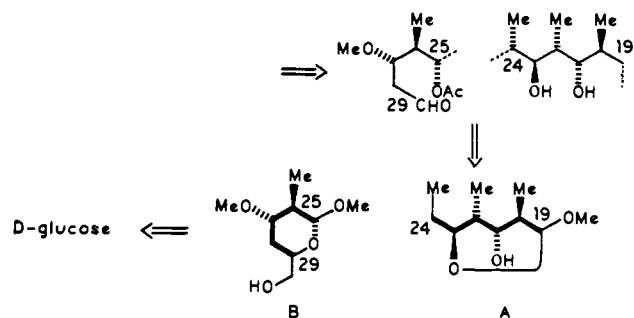
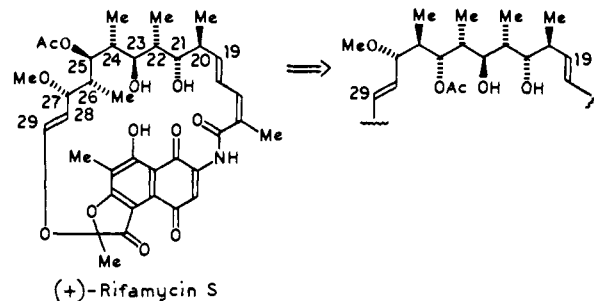
(3) See for example: (a) Corey, E. J.; Hase, T. *Tetrahedron Lett.* **1980**, 335–338. (b) Nakata, M.; Takao, H.; Ikeyama, Y.; Sakai, T.; Tatsuta, K.; Kinoshita, M. *Bull. Chem. Soc. Jpn.* **1981**, *54*, 1749–1756 and previous papers.

(4) For a recent review, see: Wehrli, W. *Top. Curr. Chem.* **1977**, *72*, 21–49 and references cited therein. See also: Prelog, V.; Oppolzer, W. *Helv. Chim. Acta* **1973**, *56*, 2279–2315.

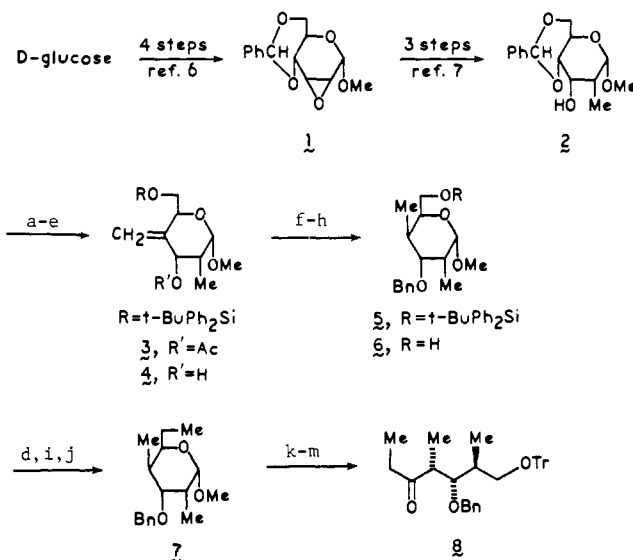
(5) Hanessian, S. *Acc. Chem. Res.* **1979**, *12*, 159–165.

(6) Wiggins, L. F. *Methods Carbohydr. Chem.* **1963**, *2*, 188–191.

Scheme I



Scheme II^a



^a Key: (a) Ac_2O , CH_2Cl_2 , DMAP, 91%; (b) 50% aqueous AcOH; (c) diphenyl-*tert*-butylsilyl chloride pyridine, 0 °C, 18 h, 88% (two steps); (d) COCl_2 , Me_2SO , CH_2Cl_2 , Et_3N , -60 to 25 °C, quantitative; (e) $\text{Ph}_3\text{P}=\text{CH}_2$, toluene, then KCN, MeOH, 88%; (f) 20% $\text{Pd}(\text{OH})_2/\text{C}, \text{H}_2$, dioxane, then BnBr, THF, KH, 92%; (g) flash chromatography, EtOAc-hexanes 15:85; (h) $n\text{-Bu}_4\text{NF}$, THF, 76%; (d) 86%; (i) $\text{Ph}_3\text{P}=\text{CH}_2$, toluene, 87.5%; (j) 5% $\text{Rh}/\text{Al}_2\text{O}_3$, H_2 , toluene, quantitative; (k) 25% aqueous AcOH, 50 °C, 1 h, then NaBH_4 , EtOH, 86%; (l) TrCl , pyridine, 65 °C, 20 h, 92%; (m) pyridinium chlorochromate, CH_2Cl_2 , 4-Å sieves; see: Herscovici, J.; Antonaki, K. *J. Chem. Soc. Chem. Commun.* **1980** 561.

was converted into **2** by methodology developed in our assembly of the erythronolide A secoacid skeleton.^{7,8} Elaboration of the

(7) Hanessian, S.; Rancourt, G.; Guindon, Y. *Can. J. Chem.* **1978**, *56*, 1843–1846. Hanessian, S.; Rancourt, G. *Ibid.* **1977**, *55*, 1111–1113. Hanessian, S.; Rancourt, G. *Pure Appl. Chem.* **1977**, *49*, 1201–1214.

(8) Satisfactory elemental analyses and spectroscopic data were obtained for new compounds reported herein. Optical rotations were measured in chloroform at concentrations of 1%. NMR spectra were recorded on Bruker 90 MHz and 400 MHz spectrometers. Mass spectra were recorded on an MM-1212 low-resolution (chemical ionization) and an MS-902 high-resolution (electron impact) instruments.